

Harnessing self-labeling enzymes for selective and concurrent A-to-I and C-to-U RNA base editing

Anna S. Stroppe¹, Ngadhnjim Latifi¹, Alfred Hanswillemeke¹,
Rafail Nikolaos Tasakis^{2,3}, F. Nina Papavasiliou^{2,3} and Thorsten Stafforst^{1,*}

¹Interfaculty Institute of Biochemistry, University of Tübingen, Auf der Morgenstelle 15, 72076 Tübingen, Germany,

²Division of Immune Diversity (D150), German Cancer Research Center (DKFZ), 69120 Heidelberg, Germany and

³Faculty of Biosciences, University of Heidelberg, 69120 Heidelberg, Germany

Received November 03, 2020; Revised May 05, 2021; Editorial Decision June 07, 2021; Accepted June 18, 2021

ABSTRACT

The SNAP-ADAR tool enables precise and efficient A-to-I RNA editing in a guideRNA-dependent manner by applying the self-labeling SNAP-tag enzyme to generate RNA-guided editases in cell culture. Here, we extend this platform by combining the SNAP-tagged tool with further effectors steered by the orthogonal HALO-tag. Due to their small size (ca. 2 kb), both effectors are readily integrated into one genomic locus. We demonstrate selective and concurrent recruitment of ADAR1 and ADAR2 deaminase activity for optimal editing with extended substrate scope and moderate global off-target effects. Furthermore, we combine the recruitment of ADAR1 and APOBEC1 deaminase activity to achieve selective and concurrent A-to-I and C-to-U RNA base editing of endogenous transcripts inside living cells, again with moderate global off-target effects. The platform should be readily transferable to further epitranscriptomic writers and erasers to manipulate epitranscriptomic marks in a programmable way with high molecular precision.

INTRODUCTION

After transcription, most RNA species get processed (e.g. capped, spliced, trimmed, polyadenylated) and enzymatically modified (1). Particularly wide-spread modifications include methylation (e.g. m⁶A, 2'-O-methylation), isomerization (pseudouridine) and deamination (e.g. A-to-I and C-to-U editing). Due to recent progress in deep sequencing technologies, the fundamental role of such epitranscriptomic modifications in human pathophysiology became apparent (2,3), including the biology of learning (4), development (5) and cancer (6,7). A detailed mechanistic understanding of the plethora of epitranscriptomic modifications is currently hampered by a lack of methods to ma-

nipulate transcripts in a programmable way with molecular precision (8). Fortunately, RNA transcripts are precisely addressable via Watson-Crick base pairing. Thus, a guideRNA can be applied to recruit a protein effector to a specific transcript in a site-specific manner. During the last years, various attempts focused on the engineering of RNA-guided RNA base editing effectors, specifically on A-to-I and C-to-U editing (8). As inosine is biochemically interpreted as guanosine, site-directed RNA editing enables the reprogramming of genetic information, e.g. substitution of amino acids, formation and removal of premature termination codons, which open novel avenues for drug discovery, promising to bypass technical and ethical issues related to genome editing (8). In this regard, our group developed an RNA-targeting platform based on fusion proteins of the self-labeling SNAP-tag (Figure 1A). To engineer a programmable A-to-I RNA base editor, we fused the SNAP-tag with the catalytic domain of the RNA editing enzyme ADAR (9,10), more specifically, we have used a hyperactive mutant (11), carrying a single glutamate (E) to glutamine (Q) mutation, indicated by the letter Q. In these fusions, the SNAP-tag (12) exploits its self-labeling activity to covalently attach to a guideRNA in a defined 1:1 stoichiometry by recognizing a benzylguanine (BG) moiety at the guideRNA (13). The guideRNA then addresses the editing of one specific adenosine residue in a selected transcript with high efficiency, broad codon scope, and very good precision (9). Competing RNA-targeting platforms, e.g. based on Cas proteins (14,15) or tethering approaches, have been developed for similar applications (8,10,16,17). Each approach has different strengths and weaknesses (8,10). A clear advantage of the SNAP-tag approach is its human origin, the small size, the ease of stable expression, the ease of transfecting one or multiple chemically stabilized guideRNA(s), which allows for concurrent editing (9), and the ready inclusion of photo control (18,19). Here, we extend the self-labeling RNA-targeting platform with HALO-tag fusions and characterize their abilities to recruit two different editing effectors in an orthogonal fash-

*To whom correspondence should be addressed. Tel: +49 7071 29 75376; Email: thorsten.stafforst@uni-tuebingen.de

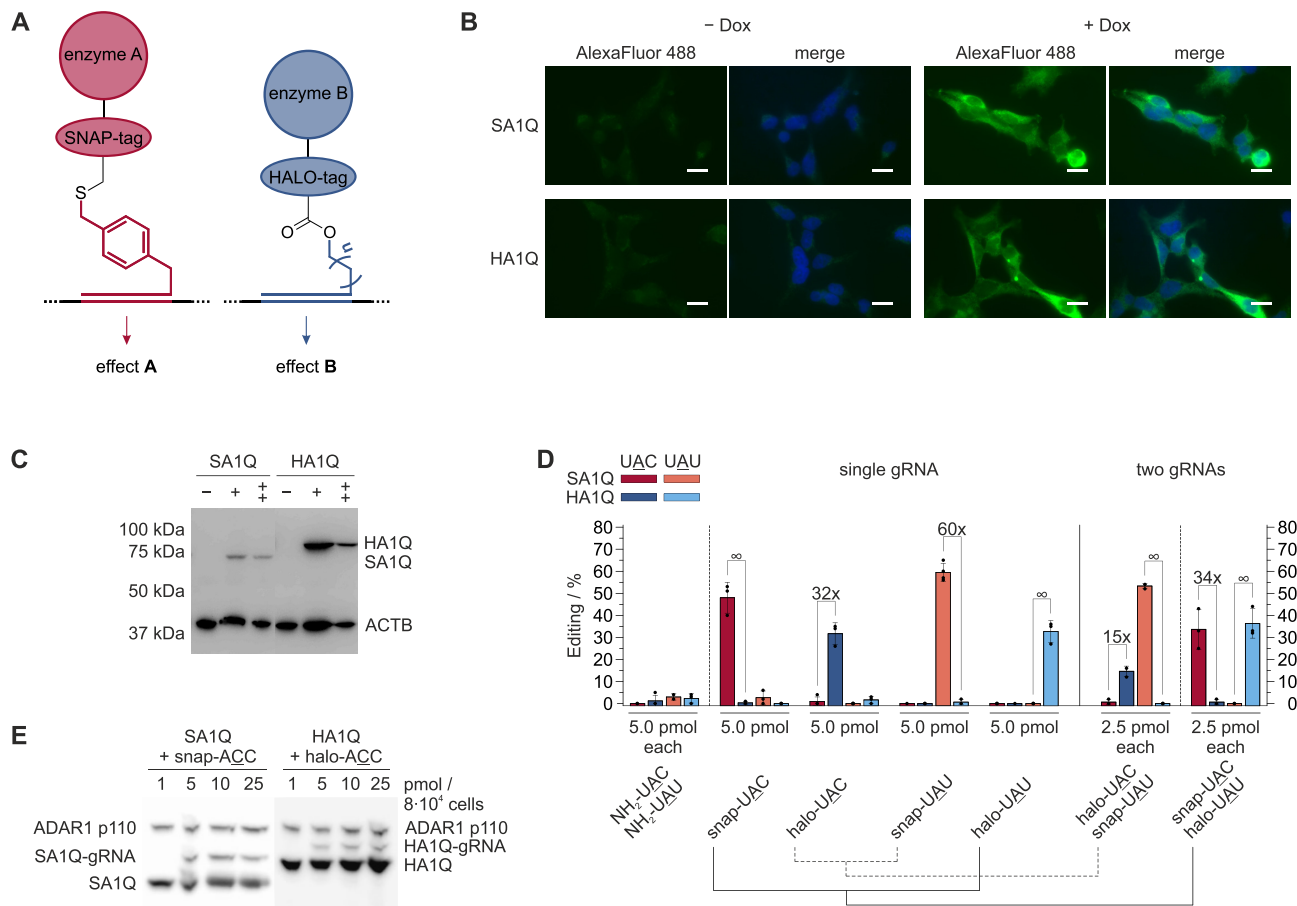


Figure 1. Recruitment of the ADAR1 deaminase domain in fusion with two different self-labeling enzymes. **(A)** Independent self-labeling enzymes, e.g. SNAP- and HALO-tag, enable for the orthogonal recruitment of various effectors, e.g. enzymes A and B. **(B)** Characterization of 293 Flp-In T-REX cell lines expressing either the Myc-tagged SA1Q or HA1Q transgene in a doxycycline-dependent fashion as visualized by immunostaining with α -Myc (green channel) and DNA staining with Hoechst 33342 (blue channel). Scale bars correspond to 15 μ m. **(C)** Western blot (α -Myc) to compare SA1Q and HA1Q expression. + means 24 h, ++ means 48 h doxycycline induction. **(D)** Editing efficiency and orthogonality of four different guideRNAs (snap-UAC, halo-UAC, snap-UAU, halo-UAU) targeting either a 5'-UAC or 5'-UAU codon in the ORF of endogenous GAPDH. Either single guideRNAs (left panel) or the indicated combination of two guideRNAs (right panel) were transfected into the SA1Q or HA1Q cell line, as indicated in the legend respectively. NH₂-guideRNAs are control guideRNAs with same sequence but lacking a self-labeling moiety. Data are shown as the mean \pm SD of $N = 3$ independent experiments. **(E)** Dose-dependent formation of SA1Q- and HA1Q-guideRNA conjugates (SA1Q-gRNA and HA1Q-gRNA) after transfection of 1.0, 5.0, 10 or 25 pmol snap- or halo-guideRNA per 8×10^4 cells respectively, visualized via Western blot (α -ADAR1). Endogenous ADAR1 p110 is equally expressed independent of guideRNA addition.

ion (Figure 1A). This broadens the otherwise limited codon scope of single editing enzymes, and enables site-selective, concurrent A-to-I and C-to-U editing within the same cell.

MATERIALS AND METHODS

Reagents and biological resources

Detailed information on reagents, enzymes, antibodies and kits as well as cell lines used in this study are presented in the Supporting Information.

Chemical synthesis

The self-labeling moieties that were attached to the guideRNAs, i.e. snap, clip, halo, halo-snap, (snap)₂ and (halo)₂ were synthesized via solid phase peptide synthesis as

described in the Supporting Information (Supplementary Schemes S1–S3, Supplementary Figures S1–S5).

Generation of guideRNAs

As guideRNAs, 22 nt long RNAs with a 5'-C6-aminolinker (NH₂-guideRNAs) that were chemically stabilized in an antagomir-like fashion as described before (20) were applied. Additional details as well as sequences and extinction coefficients at 260 nm of all used guideRNAs can be found in the Supporting Information (Supplementary Table S1).

snap-, clip- and halo-guideRNAs were produced analogous to the previously reported protocol for Npom-guideRNAs (18). Instead of N⁷-Npom-BG-Linker-COOH, 8 μ l (60 mM in DMSO, 480 nmol, \sim 35 eq) of either snap, clip or halo were used. snap- and clip-guideRNAs were purified via precipitation as described before (18). For halo-guideRNAs, samples were lyophilized after aqueous extrac-

tion from the urea PAGE and subsequently purified with C18 Reversed Phase Cartridges (WATERS, #020515) according to manufacturer's manual.

halo-snap-, (snap)₂- and (halo)₂-guideRNAs were produced analogous to the previously reported improved protocol with DIC activation (21), using 4 μl (60 mM in DMSO, 240 nmol, ~17.5 eq) of either halo-snap, (snap)₂ or (halo)₂. (snap)₂-guideRNAs were purified via precipitation as described before (21), halo-snap- and (halo)₂-guideRNAs were again purified with C18 Reversed Phase Cartridges (WATERS, #020515) according to manufacturer's manual.

Generation of stable cell lines

In general, cells were cultivated in Dulbecco's modified Eagle's medium (DMEM, LIFE TECHNOLOGIES) supplemented with 10% fetal bovine serum (FBS, LIFE TECHNOLOGIES) at 37 °C with 5% CO₂ in a water saturated steam atmosphere. For generating stable, inducible cell lines, the Flp-In™ T-REx™ system by LIFE TECHNOLOGIES was used. 4 × 10⁶ 293 Flp-In T-REx cells were seeded in 10 ml DMEM/10% FBS/100 μg/ml zeocin/15 μg/ml blasticidin (DMEM/FBS/Z/B) in a 10 cm dish. After 23 h, medium was replaced with DMEM/10% FBS (DMEM/FBS) and 1 h later 9 μg pOG 44 and 1 μg of the respective construct in a pcDNA 5 vector were forward transfected with 30 μl Lipofectamine 2000 (THERMO FISHER SCIENTIFIC). After 24 h, medium was replaced with 15 ml DMEM/10% FBS/15 μg/ml blasticidin/100 μg/ml hygromycin (DMEM/FBS/B/H), followed by selection for approximately two weeks. Then, the stable cell lines were transferred to a 75 cm² cell culture flask and subsequently cultivated in DMEM/FBS/B/H. Sequences of the constructs for all cell lines used in this study can be found in the Supporting Information.

Immunostaining of single cell lines

Briefly, 1.2 × 10⁵ SA1Q or HA1Q 293 Flp-In T-REx cells were seeded on coverslips coated with poly-D-lysine in DMEM/FBS/B/H for -Dox samples or DMEM/FBS/B/H/10 ng/ml doxycycline (DMEM/FBS/B/H/10 D) for +Dox samples respectively. After 24 h, cells were fixed with 3.7% formaldehyde in PBS, permeabilized with 1% Triton X-100 in PBS and blocked with 10% FBS in PBS. Cells were then incubated with mouse α-Myc (1:1000 in 10% FBS in PBS, SIGMA ALDRICH M4439), followed by goat α-mouse Alexa Fluor 488 (1:1000 in 10% FBS in PBS, THERMO FISHER SCIENTIFIC A11001). Nuclei were stained with NucBlue™ Live ReadyProbes™ Reagent Hoechst33342 (1:100 in PBS, THERMO FISHER SCIENTIFIC R37605) and coverslips were mounted to object slides with Fluorescence Mounting Medium by DAKO. Microscopy was performed with a ZEISS AXIO Observer.Z1 with a Colibri.2 light source under 63× magnification. For further procedural details, excitation and emission wavelengths, see Supporting Information (Supplementary Table S2).

FITC-BG & TMR-chloroalkane staining of duo cell lines

5 × 10⁴ 293 Flp-In T-REx cells from cell lines 1–5 were seeded on coverslips coated with poly-D-lysine in DMEM/FBS/B/H for -Dox samples or DMEM/FBS/B/H/10 D for +Dox samples respectively. After 24 h, cells were stained with 2 μM FITC-BG, 5 μM TMR-chloroalkane and NucBlue™ Live ReadyProbes™ Reagent Hoechst33342 (1:100, THERMO FISHER SCIENTIFIC R37605). Cells were then fixed with 3.7% formaldehyde in PBS, permeabilized with 0.1% Triton X-100 in PBS and coverslips were mounted to object slides with Fluorescence Mounting Medium by DAKO. Microscopy was performed with a ZEISS AXIO Observer.Z1 with a Colibri.2 light source under 63× magnification. For experimental data of -Dox samples, further procedural details, excitation and emission wavelengths, see Supporting Information (Supplementary Figure S6, Table S2).

Western blotting of protein expression in single cell lines

Briefly, 1 × 10⁵ SA1Q or HA1Q 293 Flp-In T-REx cells respectively were seeded and treated with doxycycline for 24 h (+) or 48 h (++) or left uninduced (-). After 48 h, cells were harvested and lysed in urea lysis buffer (8 M urea, 100 mM NaH₂PO₄, 10 mM Tris, pH 8.0) via shear force. Protein lysates were separated via SDS-PAGE and transferred onto a PVDF membrane (BIO-RAD LABORATORIES). After blocking in 5% dry milk in TBST containing 50 μg/ml avidin, the blot was incubated with mouse α-Myc (1:5000, SIGMA ALDRICH M4439) and mouse α-ACTB (1:40 000, SIGMA-Aldrich A5441) in 5% dry milk-TBST as primary antibodies. As secondary antibody, goat α-mouse HRP (1:10 000, JACKSON IMMUNORESEARCH 115-035-003) with added Precision Protein StrepTactin HRP conjugate (for visualisation of the Precision Plus Western C Standard, 1:25 000, BIO-RAD) in 5% dry milk-TBST was applied. Chemiluminescence was measured with a FUSION FX by VILBER. For full Western Blot and further experimental details, see Supporting Information (Supplementary Figure S7).

Western blotting of guideRNA-protein conjugation

2 × 10⁶ SA1Q or HA1Q 293 Flp-In T-REx cells were seeded in DMEM/FBS/B/H/10 D. After 24 h, 4 × 10⁵ cells were reverse transfected with the respective amount of snap- or halo-ACC with 2.5 μl Lipofectamine 2000. Doxycycline concentration was kept at 10 ng/ml and after further 24 h cells were lysed in 1× Laemmli (67 mM SDS, 10 mM Tris pH 6.8, 1.1 M glycerol, 0.10 M dithiothreitol, 0.15 mM bromophenol blue) in RIPA Lysis and Extraction Buffer (1% NP-40, 150 mM NaCl, 25 mM Tris-HCl pH 7.6, 1% sodium deoxycholate, 0.1% SDS, THERMO FISHER SCIENTIFIC; supplemented with 1 tablet cComplete™ Mini EDTA-free Protease Inhibitor Cocktail by ROCHE per 10 ml). Protein lysates were separated via SDS-PAGE and transferred onto a PVDF membrane (BIO-RAD LABORATORIES). After blocking in 5% dry milk in TBST, the blot was incubated with rabbit α-ADAR1 (1:1000, BETHYL LABORATORIES A303-884) and rabbit α-GAPDH (1:1000, CELL SIGNALING #5174) in 5% dry milk-TBST as primary antibodies. As

secondary antibody, goat α -rabbit HRP (1:10 000, JACKSON IMMUNORESEARCH 111-035-003) in 5% dry milk-TBST was applied. Chemiluminescence was measured with an Odyssey Fc Imaging System (LI-COR). For additional experimental data as well as further procedural details, see Supporting Information (Supplementary Figure S8).

TMR-staining & western blotting of protein expression in duo cell lines

2×10^5 293 Flp-In T-REx cells from the respective duo cell line were seeded in DMEM/FBS/B/H for -Dox samples or DMEM/FBS/B/H/10 D for +Dox samples respectively. After 24 h, cells were harvested and lysed in NP40 lysis buffer (1% NP-40, 150 mM NaCl, 50 mM Tris pH 8.0; 1 tablet cComplete™ Mini EDTA-free Protease Inhibitor Cocktail by ROCHE per 10 ml). For co-staining with TMR-BG and TMR-chloroalkane, protein lysate was incubated with 5 μ M TMR-BG and TMR-chloroalkane each in NP40 lysis buffer for 30 min at 37°C and 600 rpm. Protein lysates were then separated via SDS-PAGE and TMR-staining was visualized on a FLA 5100 by FUJIFILM with excitation at 532 nm and emission at 557 nm (Cy3 filter set). Subsequently, proteins were transferred onto a PVDF membrane (BIO-RAD LABORATORIES), and the blot was blocked in 5% dry milk in TBST containing 50 μ g/ml avidin, followed by incubation with mouse α -ACTB (1:40 000, SIGMA-Aldrich A5441), rabbit α -SNAP-tag (1:1000, NEW ENGLAND BIOLABS P9310S) and rabbit α -HaloTag (1:1000, PROMEGA G9281) in 5% dry milk-TBST as primary antibodies. As secondary antibodies, goat α -mouse HRP (1:5000, JACKSON IMMUNORESEARCH 115-035-003) with added Precision Protein StrepTactin HRP conjugate (for visualisation of the Precision Plus Western C Standard, 1:25 000, BIO-RAD) and goat α -rabbit HRP (1:5000, JACKSON IMMUNORESEARCH 111-035-003) were applied. Chemiluminescence was measured with a FUSION FX by VILBER. For additional experimental data as well as further procedural details, see Supporting Information (Supplementary Figure S9).

Editing of endogenous targets

For the editing experiments, 4×10^5 of the respective 293 Flp-In T-REx cells were seeded in DMEM/FBS/B/H/10 D. After 24 h, 8×10^4 cells were reverse transfected with the respective amount of the guideRNA to be examined with 0.5 μ l Lipofectamine 2000. Doxycycline concentration was kept at 10 ng/ml and after further 24 h (or 48 h for cell lines expressing APO1S) cells were harvested. RNA isolation was performed with the Monarch® RNA cleanup kit from NEW ENGLAND BIOLABS, followed by DNase I digestion. Samples containing (snap)₂-ACC were treated with a DNA oligonucleotide of complementary sequence (anti-(snap)₂-ACC, 1 μ M) at 95°C for 3 min to trap the guideRNA. Purified RNA was then reverse transcribed to cDNA, which was amplified via Taq PCR and subsequently analyzed with Sanger sequencing (either EUROFINS GENOMICS or MICROSYNTH). A-to-I editing yields were determined by dividing the peak height for guanosine by the sum of the peak heights for

both adenosine and guanosine. Additional experimental data and further procedural details are given in the Supporting Information (Supplementary Figures S12 and S13, Supplementary Table S3).

Editing of transfected reporter transcript

For editing of the reporter transcript, cells were forward transfected 24 h after seeding with 300 ng pcDNA 3.1 containing the coding sequence for eGFP-W58X with 1.2 μ l Lipofectamine 2000. 24 h thereafter, 8×10^4 cells were reverse transfected with the respective amount of the guideRNA to be examined with 0.5 μ l Lipofectamine 2000. Cells were harvested after further 48 h and proceeded as for editing of endogenous targets. For additional experimental data and procedural details, see Supporting Information (Supplementary Figure S14).

Next generation sequencing

For cell line 2 and 9, four samples each were prepared for NGS, i.e. a duplicate of an empty transfection and a duplicate of a guideRNA transfection (0.5 pmol (snap)₂-CAG and (halo)₂-CAU for cell line 2, 2.5 pmol (halo)₂-UAAU and (snap)₂-ACC for cell line 9), all under doxycycline induction. RNA was isolated, DNase I digested and purified via RNeasy MinElute Cleanup Kit from QIAGEN. mRNA next generation sequencing was then performed by CEGAT. The library was prepared with the library preparation kit TruSeq Stranded mRNA by ILLUMINA starting from 100 ng RNA. Samples were then sequenced on a NovaSeq 6000 by ILLUMINA with 50 million reads and 2×100 bp paired end. RNA-seq raw data from different lanes that belong to the same sample were pulled together. After adapter trimming with Trim Galore (v. 0.6.4; http://www.bioinformatics.babraham.ac.uk/projects/trim_galore/), the trimmed reads were aligned using STAR (v. 2.7.3a) (22) to a genome index inferred by the human reference genome (hg19) sequence, along with the RefSeq annotation, both publicly available at the genome browser at UCSC (23). For the alignments we considered reads that were uniquely mapped (STAR option: -outFilterMultimapNmax 1) to avoid multimapping between highly similar regions. Aligned data (bam files) were deduplicated, sorted and indexed with SAMtools (v. 1.9; <http://samtools.sourceforge.net>) (24). SNVs in our samples were called with REDIttools (v2; <https://github.com/tflati/reditools2.0>) (25,26), considering the developers' recommendations for data preparation prior to this step. Sticking to our previously published approach (9), we considered only high-quality sites (min. MeanQ > 30 in REDIttools2), and we called editing in well-covered sites (min. 50 reads in aggregate of the two replicates per sample) that showed $\geq 10\%$ (for A-to-I) or $\geq 5\%$ (for C-to-U) editing frequency when compared to the control. Additionally, fisher's exact tests were performed for all the sites that fulfilled the aforementioned criteria and significantly differentially edited sites were considered those that showed adjusted *P*-value < 0.01. Sites that were reported in the first 6 sites of a read, or in homopolymeric regions, or reported in the dbSNP (v. 142; excluding cDNA-based reported SNPs: <http://www.ncbi.nlm.nih.gov/SNP/>), were ex-

cluded throughout our output lists. All genomic coordinates were annotated with Oncotator (v1.9.9.0) (27) and Repeat Mask for Alu-SINE elements of UCSC Genome Browser (23) both for hg19. Additional data, including scatter plots of total off-targets in all editing experiments, elaborate analysis of significantly differently edited sites with editing difference $\geq 25\%$, analysis of bystander editing sites and scatter plots of all called editing sites in the two respective replicates, as well as details on the experimental procedure can be found in the Supporting Information (Supplementary Figures S16–S23, Supplementary Tables S6–S12).

RESULTS AND DISCUSSION

The HALO-tag outperforms the CLIP-tag to complement the RNA targeting platform

Two self-labeling enzymes are to be considered to complement the SNAP-tag for RNA targeting, the HALO-tag (28) and the CLIP-tag (29). The HALO-tag covalently attaches to halo-guideRNAs, carrying a 1-chloroalkane moiety (28), the CLIP-tag to clip-guideRNAs, carrying a benzylcytosine moiety for covalent conjugation (29), both in 1:1 stoichiometry. In a preliminary experiment, we identified the HALO-tag as the preferred tag for two reasons. First, a clip-guideRNA gave notable editing also with SNAP-ADAR, indicating insufficient orthogonality (29) between SNAP- and CLIP-tag in the editing application (Supplementary Figures S10–S12). Second, the clip-guideRNA showed loss of activity upon long-term storage (Supplementary Figure S12). We thus continued to compare HALO-ADAR1 (HA1Q) with SNAP-ADAR1 (SA1Q), our best RNA editor from our previous study (9). Both fusions carried the hyperactive Q mutation in the deaminase domain. Plasmid overexpression of editing enzymes typically results in enormous variability of expression levels, massive off-target editing, and low and unsteady editing efficiency at endogenous targets (10). To avoid such artefacts, we generated cell lines stably expressing either HA1Q or SA1Q from a defined, single genomic site, under control of doxycycline, by applying the 293 Flp-In T-REx system (9,19). Both cell lines expressed the respective fusion protein in a homogenous and doxycycline-inducible manner (Figure 1B). Both fusions were localized in nucleoplasm and cytoplasm, favoring the latter. The expression level of HA1Q was slightly higher compared to SA1Q (Figure 1C).

Snap- and halo-guideRNAs recruit SNAP- and HALO-fusions with high selectivity

To examine editing efficiency and orthogonality, we generated four guideRNAs and transfected them separately either into the HA1Q or SA1Q cell line. Two guideRNAs were designed to target a 5'-UAC codon in the ORF of GAPDH and were only differing in the self-labeling moiety, being either benzylguanine (12) (snap-UAC) for SNAP-tag or chloroalkane (28) (halo-UAC) for HALO-tag conjugation. Another pair of guideRNAs was equally designed to target a 5'-UAU codon in GAPDH. We observed very selective and orthogonal editing, both snap-guideRNAs elicited editing only in the SA1Q cell line as both halo-guideRNAs

did in the HA1Q cell line (Figure 1D, left panel). Furthermore, editing was reliably programmable and editing in the non-targeted codon was not observed. Even though slightly higher expressed, HA1Q was less active than SA1Q on both targets. We checked the in situ assembly of each fusion protein with its respective guideRNA by Western blot (Figure 1E). Both couples gave a similar dose-dependent formation of the protein–guideRNA conjugate not exhausting the protein component at guideRNA amounts typically applied in editing reactions. Thus, neither expression level nor conjugation efficiency explains the slightly reduced editing efficiency of HA1Q. Co-transfection of two guideRNAs, one halo- and one snap-guideRNA, gave decent editing with high selectivity for the matching enzyme in each respective cell line (Figure 1D, right panel), highlighting that the co-transfection of a guideRNA with mismatching self-labeling moiety is possible and does not interfere with the selectivity of the matching guideRNA.

Cell lines co-expressing SNAP- and HALO-tagged effectors are easily generated

Next, we explored the selective and concurrent recruitment of two different effectors based on the orthogonal self-labeling reactions mediated by SNAP- and HALO-tag within one cell (Figure 1A). As effectors, we first combined two different A-to-I RNA editing enzymes, and later one A-to-I with one C-to-U RNA editase.

ADAR1 and ADAR2 have partly complementing substrate preferences (9,30). Hence, their orthogonal recruitment inside a cell is highly desired and we decided to co-express the newly characterized HA1Q (Figure 1) with the formerly characterized (9) SA2Q. In contrast to competing RNA targeting platforms, e.g. based on Cas proteins, self-labeling proteins are of small size with only 2.2 kb for HA1Q and 1.8 kb for SA2Q. This enabled us to generate small co-expression cassettes in the pcDNA 5 backbone which allow for their targeted integration into the FRT recombination site of 293 Flp-In T-REx cells (9,19). The strong expression of two transgenes within close proximity often leads to their mutual transcriptional interference (31). Thus, we constructed five different cassettes (Figure 2A), varying the relative positioning of the two transgenes, their promoters (CMV or Efl α), and their direction of transcription. We also tested a P2A (32) fusion construct that drives both transgenes from one promoter. All five constructs were integrated into the 293 Flp-In T-REx parent cell line by simple plasmid transfection to generate duo cell lines that express both transgenes homogeneously among the cell population under doxycycline control (Figure 2B, Supplementary Figure S6). Importantly, ready-to-use duo cell lines were obtained after two weeks of antibiotic selection with no need for cumbersome clonal selection. To better characterize the relative transgene expression in duo cell lines 1–5, we stained both HA1Q and SA2Q in a defined 1:1 stoichiometry with tetramethylrhodamine (TMR) by adding TMR-benzylguanine and TMR-chloroalkane to full cell lysate and analyzed the stained proteins after SDS-PAGE separation (Figure 2C, Supplementary Figure S9). In a preliminary editing experiment, we tested for the editing activity of both transgenes in all five duo cell lines and found

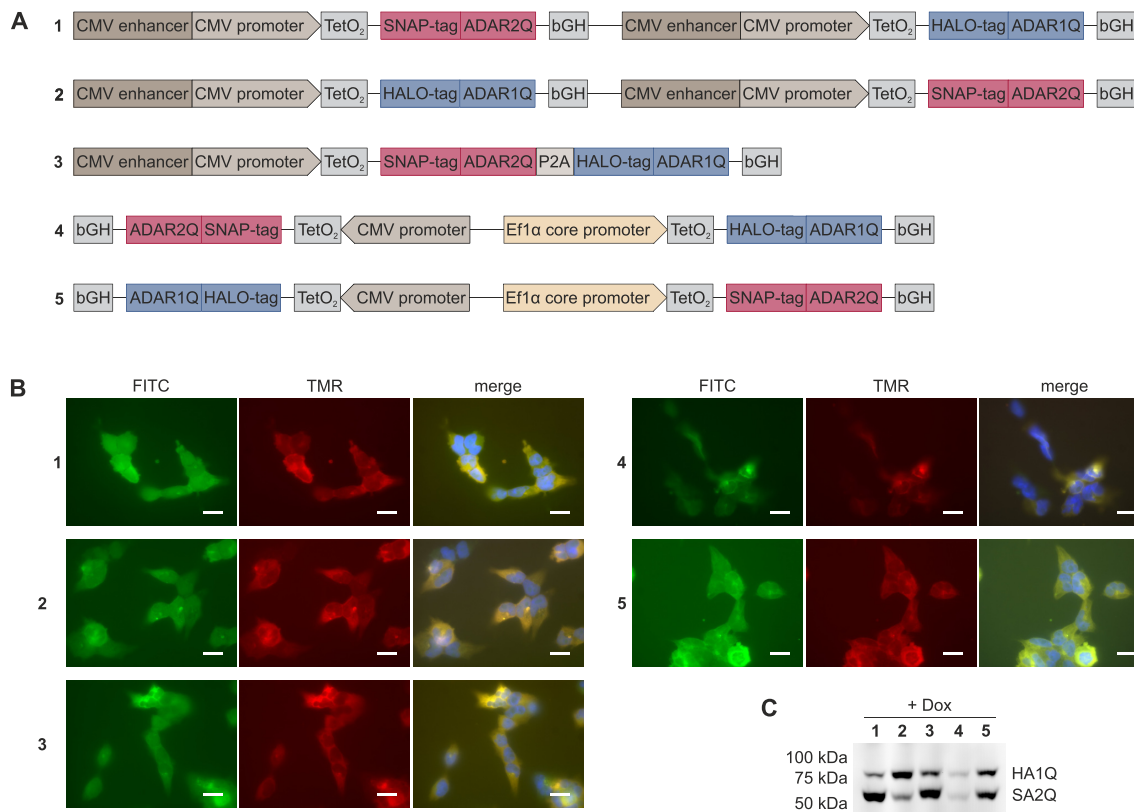


Figure 2. Generation of duo cell lines 1–5 for homogenous co-expression of two transgenes. (A) Constructs (1–5) were designed to co-express both transgenes (HA1Q and SA2Q) from one cassette under doxycycline control. TetO₂: tet operator, leads to repression of expression in the absence of a tetracycline (33); bGH: bovine growth hormone terminator; P2A: porcine teschovirus-1 self-cleaving 2A peptide (32). (B) All duo cell lines have been characterized for the transgene co-expression by staining with FITC-BG (green channel) and TMR-chloroalkane (red channel). Cell nuclei are stained with Hoechst 33342 (blue channel). Scale bars correspond to 15 μ m. (C) Characterization of relative transgene expression via SDS-PAGE after co-staining with TMR-BG and TMR-chloroalkane in raw cell lysate.

HA1Q expression to be the major limiting factor (Supplementary Table S3). We continued the study largely based on duo cell line 2, which expressed HA1Q to the highest level and SA2Q to a level sufficient to obtain good editing yields.

Selective recruitment of ADAR1 and ADAR2 activity extends the codon scope

ADAR1 and ADAR2 partly prefer different codons (34,35). We have comprehensively characterized the codon preferences of SA1Q and SA2Q before (9) and found, for example, that the 5'-CAG codon was preferentially edited by SA2Q, with a 3.3-fold higher editing yield compared to SA1Q, while the 5'-CAU codon was preferentially edited by SA1Q, with a 6.3-fold higher editing yield (Figure 3A). Thus, a cell line expressing only one of the two RNA base editors will not permit optimal editing yields in any case. In contrast, we predict that the selective recruitment of HA1Q and SA2Q with halo- and snap-guideRNAs, will enable to recruit the preferred enzyme to any substrate (matching combination, Figure 3B). Accordingly, we can predict the existence of a mismatching combination of guideRNAs that will lead to inferior editing results on both targets.

Initially, we tested this by transfection of single guideRNAs into duo cell line 2 (Figure 3C, left panel). GuideRNAs were either targeting a 5'-CAG codon in the ORF of ACTB or a 5'-CAU codon in the ORF of GAPDH. Furthermore, guideRNAs were either equipped with a BG moiety (snap-guideRNA) or with a chloroalkane moiety (halo-guideRNA) to selectively recruit SA2Q or HA1Q, respectively. Indeed, recruitment of SA2Q with the snap-CAG guideRNA always gave better editing yields for the 5'-CAG codon in ACTB than recruitment of HA1Q with the halo-CAG guideRNA. As expected, the effect was reverse for the editing of the 5'-CAU codon in GAPDH. Notably, only the halo-CAU guideRNA, selective for HA1Q, was able to induce detectable editing at all. A strength of the SNAP-ADAR platform is the ease by which the short (ca. 20 nt), chemically modified guideRNAs can be transfected into cells. In the past, we demonstrated co-transfection of up to four different guideRNAs enabling multiplexed, concurrent editing of four different substrates without loss in editing efficiency (9). Now, we co-transfected two guideRNAs, one snap- and one halo-guideRNA, either in matching or mismatching combination into cell line 2. Clearly, the matching combination gave better editing yields for both substrates (CAG, CAU) compared to the mismatching combination. Again,

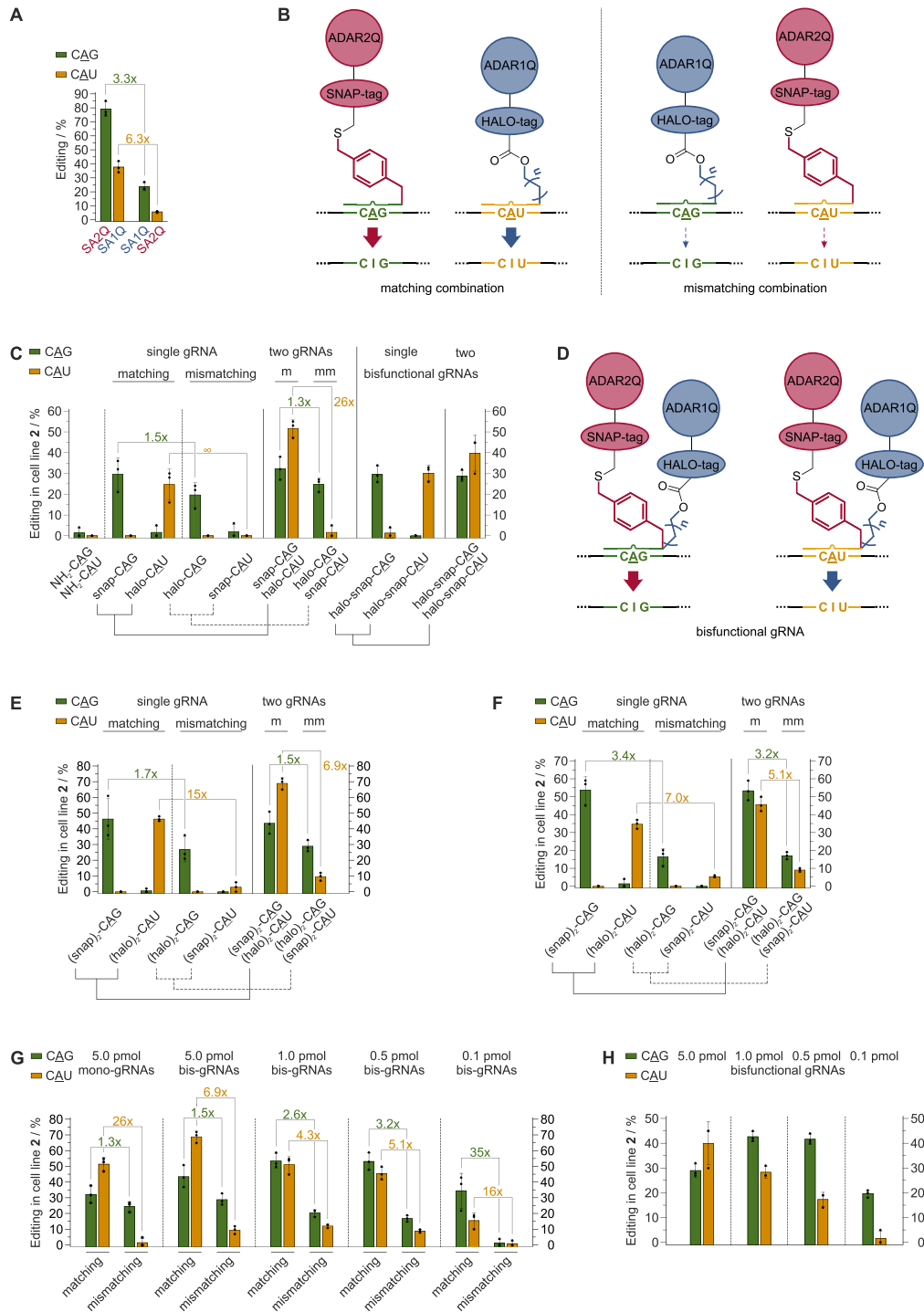


Figure 3. Editing in duo cell lines expressing HA1Q and SA2Q. (A) SA1Q and SA2Q have different preferences for 5'-CAG and 5'-CAU codons in the ORF of GAPDH, as described before (9). (B) Due to the two different self-labeling moieties (BG and chloroalkane) the SNAP-tagged ADAR2 and the HALO-tagged ADAR1 deaminase domains can be recruited either to their preferred substrates (matching combination) or to their least preferred substrates (mismatching combination). (C) Editing yield and selectivity after transfection of a single (5.0 pmol), matching or mismatching snap- or halo-guideRNA into duo cell line 2 compared to the co-transfection of two guideRNAs (one snap- and one halo-guideRNA, each 5.0 pmol) either in matching (m) or in mismatching (mm) combination (left panel). The right panel shows the activity of bisfunctional guideRNAs capable to recruit both editing enzymes with one guideRNA. (D) Bisfunctional halo-snap-guideRNAs, carrying both a chloroalkane and a BG moiety, are able to recruit both HA1Q and SA2Q, leading to maximum editing yields at any codon. (E) Editing yield and selectivity in duo cell line 2 after transfection of a single or co-transfection of two guideRNAs, one (snap)₂- and one (halo)₂-guideRNA, either in matching (m) or in mismatching (mm) combination (5.0 pmol each). (F) Same as E) but with 0.5 pmol each. (G) Concentration dependency of editing efficiency and selectivity in cell line 2 under co-transfection of (snap)₂- and (halo)₂-guideRNAs (bis-guideRNAs) in matching versus mismatching combination. For comparison, editing with the respective mono-guideRNAs (snap- and halo-guideRNAs) is shown. (H) Concentration dependency of editing yields in duo cell line 2 after co-transfection of two bisfunctional halo-snap-guideRNAs. Data in a), c), e)-h) are shown as the mean ± SD of N = 3 independent experiments.

choosing the matching combination was required to see editing with the CAU substrate at all. The same pattern was observed for a second duo cell line, cell line 5 (Supplementary Figure S13a). This demonstrates that the platform is able to target two editing enzymes independently from each other to their respective preferred target inside one cell line.

One could also conceive a bisfunctional guideRNA capable of recruiting both editases, HA1Q and SA2Q, simultaneously (Figure 3D). Such a halo-snap-guideRNA may enable maximum editing with any codon and substrate. To accomplish that, we synthesized halo-snap-guideRNAs carrying both, the BG and the chloroalkane moiety, targeting either the CAG or CAU substrate and tested them in duo cell line 2. As expected, both halo-snap-guideRNAs gave good editing yields for both codons, 5'-CAU and 5'-CAG, always resembling the editing result of the formerly preferred snap- or halo-guideRNA, respectively (Figure 3C, right panel). This clearly indicates that both enzymes have been active on the substrates.

As controls, we had also synthesized (snap)₂- and (halo)₂-guideRNAs carrying either two benzylguanine or two chloroalkane moieties, respectively. Notably, editing yields have been higher with such controls (Figure 3E, F) compared to the respective guideRNAs carrying only one self-labeling moiety. This boost might be due to the recruitment of two instead of one editing enzyme per guideRNA. Similar effects have been described in the context of other RNA editing systems before (36). Interestingly, not only the yield but also the selectivity (e.g. CAG codon) was better than before (Figure 3F). One can expect that the selectivity increases further if one reduces the concentration of the guideRNA-enzyme conjugate inside the cell. Thus, we varied the amount of the two transfected guideRNAs (one (snap)₂- and one (halo)₂-guideRNA, either matching or mismatching) between 5 pmol and 0.1 pmol in four steps (Figure 3G, Supplementary Figure S13b, c). Indeed, stepwise reduction of the guideRNA amount improved the selectivity progressively. At 0.1 pmol guideRNA, excellent selectivity was obtained with virtually no residual editing on both targets (CAG and CAU) in the mismatching combination. Notably, the editing yields were satisfying also at low amounts of guideRNA. A similar trend, but with lower editing yields, was seen for the bisfunctional halo-snap-guideRNAs (Figure 3H, Supplementary Figure S13d) indicating that the recruitment of two copies of the preferred editing enzyme gives better editing yield than the co-recruitment of one preferred and one non-preferred enzyme.

Genomic co-expression of two editing enzymes elicits moderate global off-target editing

Overexpression of engineered, highly active editing enzymes leads to significant off-target editing throughout the whole transcriptome (8,10). Various strategies have been tried to minimize this (8,10). In this regard, we demonstrated that the controlled expression of SA1Q and SA2Q from single genomic loci reduces global off-target editing tremendously (9). We now determined the total off-target editing in duo cell line 2 after co-transfection with 0.5 pmol (snap)₂-CAG

Table 1. Number of significantly differently edited sites found in editing experiments in mono cell lines SA1Q, SA2Q, and in duo cell line 2 (HA1Q + SA2Q) in comparison to a negative control cell line (293 Flp-In T-REx) not expressing any editing enzyme (Total off-targets). The last column shows the guideRNA-dependent fraction of the total off-targets for duo cell line 2

	Total off-targets		gRNA-dependent	
	SA1Q	SA2Q	HA1Q + SA2Q	HA1Q + SA2Q
Total number	3406	4795	8391	653
incl. Alu sites	400	1190	1281	136
5'UTR	124	168	286	19
Missense mutation	769	1080	2150	166
Nonstop mutation	51	46	108	5
Start codon SNP	1	1	2	0
Silent	470	515	1079	74
3'UTR	1427	2009	3422	267
Noncoding	564	976	1343	122

and 0.5 pmol (halo)₂-CAU guideRNA, by determining significantly differently edited sites in comparison with a negative control expressing no artificial editing enzyme. As the pipeline was more sensitive than the one used before (9), we re-analyzed the raw data of the total off-target editing for mono cell lines expressing SA1Q or SA2Q, in presence of an ACTB-targeting snap-guideRNA (9), with the new pipeline to allow for direct side-by-side comparison with duo cell line 2. With 8391 sites, the amount of total off-target editing in duo cell line 2 roughly comprised the aggregate of sites found in mono cell lines SA1Q and SA2Q (Table 1, Figure 4A, Supplementary Figure S16). However, the vast majority of editing sites (ca. 75%) showed changes in editing levels below 25% (Supplementary Table S6, Figure 4A). The total off-targets comprise guideRNA-dependent and -independent editing events. To determine the guideRNA-dependent fraction we compared the off-target editing for cell line 2 with versus without co-transfection of the two guideRNAs. Our sensitive pipeline detected 653 sites that were significantly differently edited depending on the presence of the guideRNAs (Figure 4B, Table 1). Again, only a small number of sites (Supplementary Table S6) showed editing sites with levels elevated above 25%. Among these 37 sites, only five sites were missense mutations. After careful analysis, almost all 37 sites could be assigned to either binding of the GAPDH or ACTB guideRNA, respectively (Supplementary Figures S17–S19). Notably, only one missense mutation (ACTA2, 47%) achieved editing levels similar to the on-targets GAPDH (41%) and ACTB (52%), see Supplementary Table S7. This was due to the high sequence homology between ACTA2 and ACTB. In order to spot even minute guideRNA-dependent bystander editings, we manually analyzed the regions around the two on-target sites (\pm 500 bp) without applying the usual cutoff for editing difference. This yielded 4 bystander sites in GAPDH (editing difference \leq 1%) and 10 sites in ACTB, with the three highest sites exhibiting editing differences between 16.0% and 7.7%, likely due to high similarity with the on-target site (Supplementary Tables S8 and S9, Supplementary Figure S20). Overall, NGS analysis demonstrated again (9,10) that total off-target effects are dominated by guideRNA-

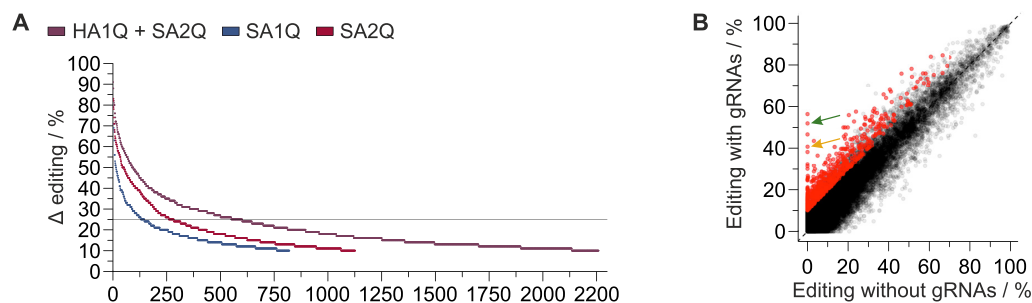


Figure 4. Off-target analysis of duo cell line 2. (A) Total off-target editing of duo cell line 2 (HA1Q + SA2Q) in comparison with mono cell lines SA1Q and SA2Q. Shown are significantly differently edited sites ($\geq 10\%$ editing difference, Fisher's exact test, two-sided, adjusted $P < 0.01$, $n = 2$ experiments) that led to nonsynonymous substitutions, sorted by editing difference. (B) Scatter plot depicting the guideRNA-dependent off-target effects in duo cell line 2. Significantly differently edited sites are marked in red. The two on-target sites (in ACTB and GAPDH) are marked by a green and yellow arrow respectively.

independent off-target effects rather than by mis-guiding through the guideRNAs.

Selective site-directed C-to-U and A-to-I editing can be combined within one cell

C-to-U and A-to-I RNA base editing complement one another. While A-to-I editing can remove premature STOP codons, C-to-U editing can write them and furthermore affect different amino acid substitutions, including key residues like serine and proline. APOBEC1-mediated C-to-U RNA editing plays a key role for human physiology by inducing an isoform switch in ApoB48/100 (37). In preliminary experiments, we found that a simple fusion of the SNAP-tag to the C-terminus of murine APOBEC1 generates an effector protein dubbed APO1S that can induce C-to-U editing in an RNA-guided manner. Fully analog to the duo cell lines above, we generated four duo cell lines (6–9, Figure 5A) that co-express the HA1Q and APO1S transgenes under control of doxycycline. Via western blot/SDS PAGE we characterized the relative transgene expression (Figure 5B), which suggested cell line 6 and 9 to express sufficient levels of both effectors. Notably, the inserts of cell lines 6 and 9 are constructed analog to those in cell lines 2 and 5, indicating that these two designs might be generally applicable for the co-expression of two RNA-guided effector proteins.

A first set of editing experiments targeted a 5'-UAG codon for HA1Q-mediated A-to-I editing and a proximal 5'-ACG codon for APO1S-mediated C-to-U editing in an eGFP reporter transcript in duo cell line 9. The target sites are close enough to design one guideRNA that can mediate both, adenosine or cytidine deamination, depending on the self-labeling moiety attached, since HA1Q requires an RNA duplex as substrate (9) whereas APO1S prefers its positioning 4–6 nt upstream of the target site (Figure 5C). As expected, the halo-eGFP guideRNA elicited A-to-I editing, the snap-eGFP guideRNA elicited C-to-U editing and a bisfunctional halo-snap-eGFP guideRNA induced both A-to-I and C-to-U editing (Figure 5D). Similar results have been obtained in the cell lines 6 and 7 (Supplementary Figure S14). Notably, the snap-eGFP guideRNA also induced some A-to-I editing. However, highly selective C-to-U editing was achieved when a snap-eGFP guideRNA

was applied that was fully chemically modified (*mod-snap-eGFP*, Figure 5C, Supplementary Table S1) and that did not contain the modification gap (38) around the adenosine required for ADAR1 action (Figure 5D). This highlights another strength of the RNA targeting platform. Bystander off-target editing can be easily controlled by chemical modification of the guideRNA (9), a frequent problem (8,10) with RNA base editing approaches that apply genetically encoded guideRNAs.

In a second set of editing experiments, we applied two different guideRNAs to selectively recruit APO1S and HA1Q to two different endogenous transcripts in duo cell line 9. The (halo)₂-UAU guideRNA steers HA1Q to edit the adenosine in a 5'-UAU codon in the ORF of ACTB, the (snap)₂-ACC guideRNA steers APO1S to edit the cytosine in a 5'-ACC codon in the ORF of GAPDH (Figure 5E). In contrast to the editing of the eGFP reporter, editing on endogenous ORF targets was very selective. The (halo)₂-UAU guideRNA induced site-specific A-to-I editing with excellent yields (ca. 65%) in the ACTB transcript with no detectable C-to-U editing, whereas the (snap)₂-ACC guideRNA induced site-specific C-to-U editing with moderate yield (ca. 20%) in the GAPDH transcript, again with no detectable A-to-I RNA editing (Figure 5F). Notably, co-transfection of both guideRNAs induced selective A-to-I and C-to-U editing in the ACTB and GAPDH transcript, respectively, without any loss of editing efficiency compared to the single guideRNA transfections. Similar results have been obtained in the cell lines 6 and 7 (Supplementary Figure S13e). Thus, concurrent C-to-U and A-to-I editing can be done within one cell under programmable target selection.

We then benchmarked the C-to-U editing efficiency achieved with APO1S in duo cell line 9 at both targets (eGFP and GAPDH) with the recently published (39) Cas13-based RESCUE approach (Supplementary Figure S15). Specifically, we tested the most active variant, RESCUer16, and tried four different C-flip guideRNAs for each target (Supplementary Table S4). The APO1S enzyme outcompeted RESCUer16 on both targets with respect to on-target editing yield. While we found C-to-U bystander editing for both approaches, only the RESCUE approach induced A-to-I bystander editing (Supplementary Table S5).

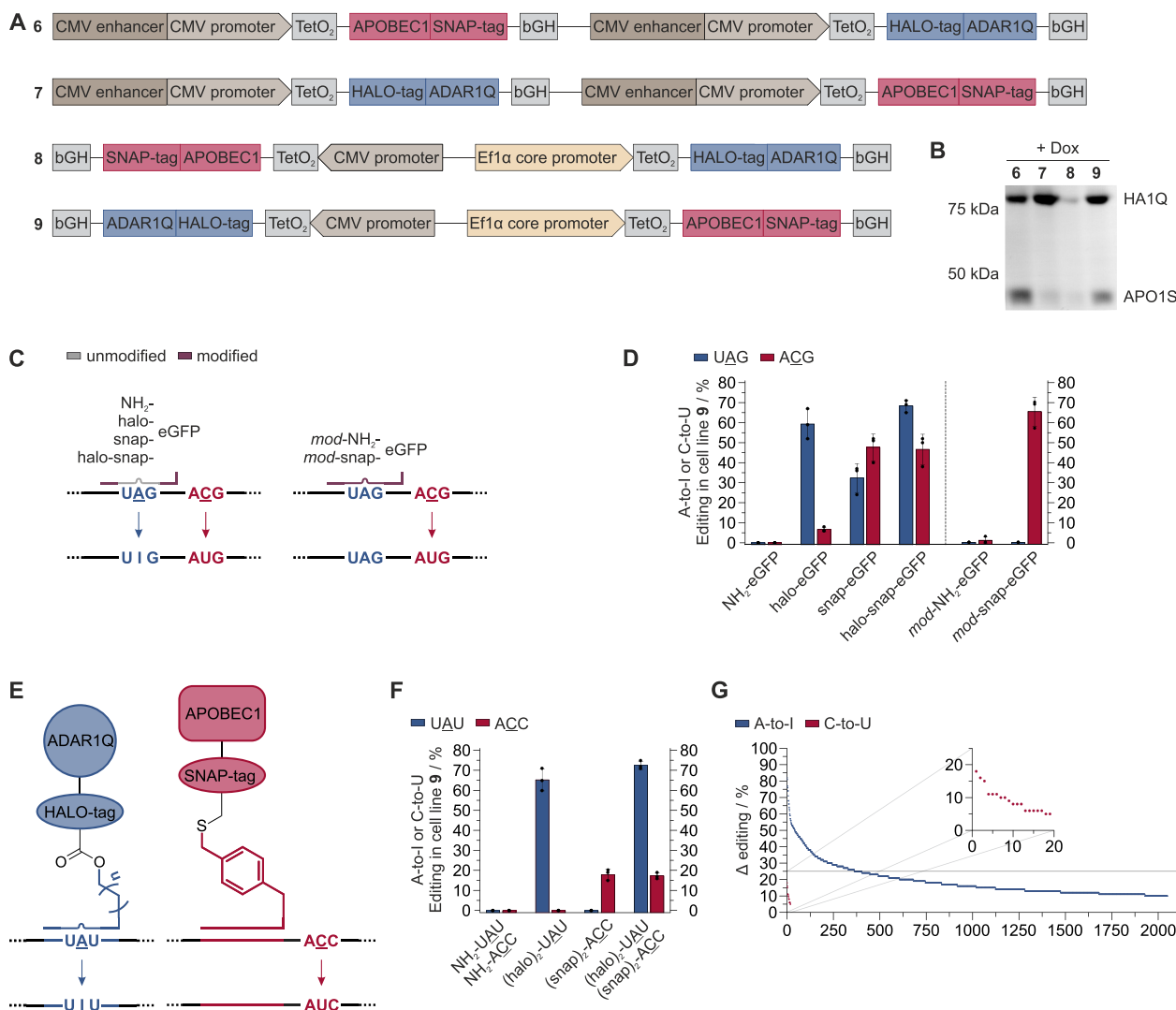


Figure 5. Selective and concurrent A-to-I and C-to-U editing. (A) Constructs (6-9) were designed to co-express both transgenes (APO1S and HA1Q) from one cassette under doxycycline control. TetO₂: tet operator, leads to repression of expression in the absence of a tetracycline (33); bGH: bovine growth hormone terminator; P2A: porcine teschovirus-1 self-cleaving 2A peptide (32). (B) Characterization of relative transgene expression via SDS-PAGE after co-staining with TMR-BG and TMR-chloroalkane in raw cell lysate. (C) GuideRNA design to enable or block concurrent A-to-I and C-to-U editing in an eGFP reporter with a single guideRNA. The modified guideRNA (*mod-snap-eGFP*) contained chemical modifications (Supplementary Table S1) that block A-to-I editing. (D) Editing yield in cell line 9 from concurrent A-to-I and C-to-U editing in an eGFP reporter transcript after transfection of a halo-, snap- or halo-snap-guideRNA (5.0 pmol). (E) GuideRNA design and recruiting strategy for concurrent and selective A-to-I and C-to-U editing at two different endogenous transcripts. (F) Editing yield in cell line 9 for selective and concurrent editing as depicted in E after transfection of a single or co-transfection of two guideRNAs, one (halo)₂-guideRNA for A-to-I editing in ACTB and one (snap)₂-guideRNA for C-to-U editing in GAPDH (5.0 pmol each). Data in D) and F) are shown as the mean ± SD of N = 3 independent experiments. (G) Total off-target A-to-I and C-to-U editing of duo cell line 9. Shown are significantly differently edited sites (for A-to-I ≥ 10% editing difference, for C-to-U ≥ 5% editing difference, Fisher's exact test, two-sided, adjusted P < 0.01, n = 2 experiments) that led to nonsynonymous substitutions, sorted by editing difference. A-to-I (in ACTB) and C-to-U (in GAPDH) on-target sites are no. 40 and no. 18, respectively.

To assess transcriptome-wide global A-to-I and C-to-U off-target editing, we applied next generation RNA sequencing to detect significantly differently edited sites in duo cell line 9 after co-transfection of 2.5 pmol (halo)₂-UAU and 2.5 pmol (snap)₂-ACC guideRNA in comparison to a cell line lacking expression of any artificial editing enzyme (Table 2, Figure 5g, Supplementary Figure S22). Expressing only one A-to-I editing enzyme (HA1Q), the total number of A-to-I off-target sites (6767) was below that of duo cell line 2, which expresses two A-to-I editing enzymes.

Again, the majority of sites exhibited differences in editing below 25% (Supplementary Table S10). A slightly higher fraction of the off-target sites was guideRNA-dependent compared to cell line 2, which might be due to the higher guideRNA amounts applied in cell line 9. However, in particular off-target sites with high editing differences, e.g. ≥ 25%, were typically guideRNA-independent (Supplementary Table S10). Taking the generally lower C-to-U editing yields into account, we adapted the pipeline and set the cutoff for editing differences to 5%. With this highly sen-

Table 2. Number of significantly differently edited A-to-I and C-to-U sites found in editing experiments in duo cell line **9** (HAIQ + APO1S) in comparison to a negative control cell line (293 Flp-In T-REx) not expressing any editing enzyme (Total off-targets). The guideRNA-dependent fractions of the total off-targets are shown in the right column, respectively

	A-to-I ($\Delta \geq 10\%$)		C-to-U ($\Delta \geq 5\%$)	
	Total off-targets	gRNA-dependent	Total off-targets	gRNA-dependent
Total number incl. Alu sites	6767 729	2148 85	2976 17	153 1
5'UTR	262	92	44	3
Missense mutation	1944	704	16	1
Nonsense mutation	0	0	2	0
Nonstop mutation	104	30	0	0
Start codon SNP	2	0	0	0
Silent	979	352	17	2
3'UTR	2560	731	2593	131
Noncoding	916	239	304	16

sitive pipeline, we were able to find 2976 significantly differently edited sites (Table 2). However, the vast number of sites showed editing differences below 10%, and only 129 sites had editing differences above 25% (Supplementary Table S11). Notably, almost all off-target sites were located in the 3'-UTR, and only 18 of 2976 total sites were inducing missense or nonsense mutations. Also the number of guideRNA-dependent off-targets sites was comparably low (153 of 2976), with basically all in the 3'-UTR (Table 2, Supplementary Table S11). Again, we manually analyzed the regions (± 500 bp) around the on-target site to detect low-level bystander A-to-I editing in ACTB (Supplementary Table S13) and C-to-U bystander editing in GAPDH (Supplementary Table S12). We found one bystander site in ACTB (editing difference $\leq 1\%$) and a larger number (22) of bystander sites in GAPDH, but only one of the 22 sites had an editing difference $\geq 1\%$. Overall, our approach for concurrent A-to-I and C-to-U RNA editing, based on co-expression of two different editing enzymes gave moderate, mainly guideRNA-independent off-target effects for both effectors.

CONCLUSIONS

Here, we show for the first time that one can combine two self-labeling enzymes to create a powerful RNA targeting platform to manipulate RNA inside living cells in a yet unprecedented way. The orthogonality of HALO- and SNAP-tag sets the ground for the selective and programmable steering of two different RNA effectors. Furthermore, the approach benefits from the small size of the fusion proteins, which enable their facile genomic co-integration, and the ease by which the short (20 nt), chemically stabilized guideRNAs can be co-transfected and optimized to reduce bystander editing, if required. Recent attempts to combine two base editing activities in one protein either to target DNA (40) or RNA (39) illustrate the manifold problems of controlling two enzyme functions independently, which we could solve here for RNA base editing. We successfully demonstrate the functioning of our approach for the orthogonal and concurrent recruitment of two pairs of editing effectors. The selective recruitment of ADAR1 and

ADAR2 deamination activity enables site-directed A-to-I RNA base editing with improved editing efficiency. The selective recruitment of ADAR1 and APOBEC1 deamination activity allows for target-selective, concurrent A-to-I and C-to-U editing. Notably, orthogonality is particularly effective with guideRNAs that can recruit two copies of an editase. Again, we demonstrate that genetic integration of the editing enzymes helps to control global off-target A-to-I and C-to-U editing induced by unengaged editing enzymes (9,10,16,41). Notably, even the concurrent transfection of two guideRNAs leads to only a very small number of off-target editing events caused by misguiding through the guideRNAs, and might be amenable for further sequence optimization, if required.

Furthermore, our platform benefits from the high flexibility in the linker chemistry. This makes it possible to control the composition and stoichiometry of two fusion proteins at a target with one guideRNA. We exemplify this with the generation of bisfunctional guideRNAs that are capable of co-recruiting either ADAR1/ADAR2 or ADAR1/APOBEC1 to one target with one guideRNA. The possibility of including photochemistry to the linker may add another level of spatio-temporal control in the future (18,19). The general concept we present here may be readily transferred to recruit further pairs of writers and erasers of epitranscriptomic marks with ease and unprecedented control (2,42,43).

DATA AVAILABILITY

NGS raw data for duo cell lines **2** and **9** can be found on NCBI GEO under GSE160945. The online Supplementary Information contains an excel sheet with all editing yields, an excel sheet with the NGS analysis, SnapGene files for all transgenic constructs, and a PDF file giving detailed information on syntheses, protocols, and additional experimental data.

SUPPLEMENTARY DATA

Supplementary Data are available at NAR Online.

FUNDING

Deutsche Forschungsgemeinschaft (DFG, German Research Foundation) [430214260, STA1053/7-1 to T.S.]; DFG priority program SPP 1784 [404867268 to F.N.P., T.S.]; European Research Council (ERC) under the European Union's Horizon 2020 research and innovation program [649019 to F.N.P., 647328 to T.S.]. Funding for open access charge: ERC; DFG.

Conflict of interest statement. T.S. holds patents on site-directed RNA editing.

REFERENCES

- Corbett, A.H. (2018) Post-transcriptional regulation of gene expression and human disease. *Curr. Opin. Cell Biol.*, **52**, 96–104.
- Kadumuri, R.V. and Janga, S.C. (2018) Epitranscriptomic code and its alterations in human disease. *Trends Mol. Med.*, **24**, 886–903.
- Gagnidze, K., Rayon-Estrada, V., Harroch, S., Bulloch, K. and Papavasiliou, F.N. (2018) A new chapter in genetic medicine: RNA

- editing and its role in disease pathogenesis. *Trends Mol. Med.*, **24**, 294–303.
4. Shi, H., Zhang, X., Weng, Y.-L., Lu, Z., Liu, Y., Lu, Z., Li, J., Hao, P., Zhang, Y., Zhang, F. *et al.* (2018) m⁶A facilitates hippocampus-dependent learning and memory through YTHDF1. *Nature*, **563**, 249–253.
 5. Frye, M., Harada, B.T., Behm, M. and He, C. (2018) RNA modifications modulate gene expression during development. *Science*, **361**, 1346–1349.
 6. Liu, J., Eckert, M.A., Harada, B.T., Liu, S.-M., Lu, Z., Yu, K., Tienda, S.M., Chryplewicz, A., Zhu, A.C., Yang, Y. *et al.* (2018) m⁶A mRNA methylation regulates AKT activity to promote the proliferation and tumorigenicity of endometrial cancer. *Nat. Cell Biol.*, **20**, 2085–2083.
 7. Ishizuka, J.J., Manguso, R.T., Cheruiyot, C.K., Bi, K., Panda, A., Iracheta-Vellve, A., Miller, B.C., Du, P.P., Yates, K.B., Dubrot, J. *et al.* (2019) Loss of ADAR1 in tumours overcomes resistance to immune checkpoint blockade. *Nature*, **565**, 43–48.
 8. Rees, H.A. and Liu, D.R. (2018) Base editing: precision chemistry on the genome and transcriptome of living cells. *Nat. Rev. Genet.*, **19**, 770–788.
 9. Vogel, P., Moschref, M., Li, Q., Merkle, T., Selvasarayanan, K.D., Li, J.B. and Stafforst, T. (2018) Efficient and precise editing of endogenous transcripts with SNAP-tagged ADARs. *Nat. Methods*, **15**, 535–538.
 10. Vogel, P. and Stafforst, T. (2019) Critical review on engineering deaminases for site-directed RNA editing. *Curr. Opin. Biotechnol.*, **55**, 74–80.
 11. Kuttan, A. and Bass, B.L. (2012) Mechanistic insights into editing-site specificity of ADARs. *Proc. Natl. Acad. Sci. U.S.A.*, **109**, E3295–E3304.
 12. Keppler, A., Gendreizig, S., Gronemeyer, T., Pick, H., Vogel, H. and Johnsson, K. (2003) A general method for the covalent labeling of fusion proteins with small molecules *in vivo*. *Nat. Biotechnol.*, **21**, 86–89.
 13. Stafforst, T. and Schneider, M.F. (2012) An RNA–Deaminase conjugate selectively repairs point mutations. *Angew. Chem.*, **124**, 11329–11332.
 14. Abudayyeh, O.O., Gootenberg, J.S., Konermann, S., Joung, J., Slaymaker, I.M., Cox, D.B.T., Shmakov, S., Makarova, K.S., Semenova, E., Minakhin, L. *et al.* (2016) C2c2 is a single-component programmable RNA-guided RNA-targeting CRISPR effector. *Science*, **353**, 5573.
 15. Abudayyeh, O.O., Gootenberg, J.S., Essletzbichler, P., Han, S., Joung, J., Belanto, J.J., Verdine, V., Cox, D.B.T., Kellner, M.J., Regev, A. *et al.* (2017) RNA targeting with CRISPR–Cas13. *Nature*, **550**, 280–284.
 16. Cox, D.B.T., Gootenberg, J.S., Abudayyeh, O.O., Franklin, B., Kellner, M.J., Joung, J. and Zhang, F. (2017) RNA editing with CRISPR–Cas13. *Science*, **358**, 1019–1027.
 17. Montiel-Gonzalez, M.F., Vallecillo-Viejo, I., Yudowski, G.A. and Rosenthal, J.J.C. (2013) Correction of mutations within the cystic fibrosis transmembrane conductance regulator by site-directed RNA editing. *Proc. Natl. Acad. Sci. U.S.A.*, **110**, 18285–18290.
 18. Hanswillemenke, A., Kuzdere, T., Vogel, P., Jékely, G. and Stafforst, T. (2015) Site-directed RNA editing *in vivo* can be triggered by the light-driven assembly of an artificial riboprotein. *J. Am. Chem. Soc.*, **137**, 15875–15881.
 19. Vogel, P., Hanswillemenke, A. and Stafforst, T. (2017) Switching protein localization by site-directed RNA editing under control of light. *ACS Synth. Biol.*, **6**, 1642–1649.
 20. Vogel, P. and Stafforst, T. (2014) Site-directed RNA editing with antagomir deaminases — a tool to study protein and RNA function. *ChemMedChem*, **9**, 2021–2025.
 21. Hanswillemenke, A. and Stafforst, T. (2019) Protocols for the generation of caged guideRNAs for light-triggered RNA-targeting with SNAP-ADARs. *Methods Enzymol.*, **624**, 47–68.
 22. Dobin, A., Davis, C.A., Schlesinger, F., Drenkow, J., Zaleski, C., Jha, S., Batut, P., Chaisson, M. and Gingeras, T.R. (2013) STAR: ultrafast universal RNA-seq aligner. *Bioinformatics*, **29**, 15–21.
 23. Kent, W.J., Sugnet, C.W., Furey, T.S., Roskin, K.M., Pringle, T.H., Zahler, A.M. and Haussler, D. (2002) The human genome browser at UCSC. *Genome Res.*, **12**, 996–1006.
 24. Li, H., Handsaker, B., Wysoker, A., Fennell, T., Ruan, J., Homer, N., Marth, G., Abecasis, G. and Durbin, R. (2009) The sequence alignment/map format and SAMtools. *Bioinformatics*, **25**, 2078–2079.
 25. Lo Giudice, C., Tangaro, M.A., Pesole, G. and Picardi, E. (2020) Investigating RNA editing in deep transcriptome datasets with REDIttools and REDIportal. *Nat. Protoc.*, **15**, 1098–1131.
 26. Picardi, E. and Pesole, G. (2013) REDIttools: high-throughput RNA editing detection made easy. *Bioinformatics*, **29**, 1813–1814.
 27. Ramos, A.H., Lichtenstein, L., Gupta, M., Lawrence, M.S., Pugh, T.J., Saksena, G., Meyerson, M. and Getz, G. (2015) Oncotator: cancer variant annotation tool. *Hum. Mutat.*, **36**, E2423–E2429.
 28. Los, G.V., Encell, L.P., McDougall, M.G., Hartzell, D.D., Karassina, N., Zimprich, C., Wood, M.G., Learish, R., Ohana, R.F., Urh, M. *et al.* (2008) HaloTag: a novel protein labeling technology for cell imaging and protein analysis. *ACS Chem. Biol.*, **3**, 373–382.
 29. Gautier, A., Juillerat, A., Heinis, C., Corrêa, I.R. Jr, Kindermann, M., Beaufile, F. and Johnsson, K. (2008) An engineered protein tag for multiprotein labeling in living cells. *Chem. Biol.*, **15**, 128–136.
 30. Eggington, J.M., Greene, T. and Bass, B.L. (2011) Predicting sites of ADAR editing in double-stranded RNA. *Nat. Commun.*, **2**, 319–319.
 31. Palmer, A.C., Egan, J.B. and Shearwin, K.E. (2011) Transcriptional interference by RNA polymerase pausing and dislodgement of transcription factors. *Transcription*, **2**, 9–14.
 32. Kim, J.H., Lee, S.-R., Li, L.-H., Park, H.-J., Park, J.-H., Lee, K.-Y., Kim, M.-K., Shin, B.A. and Choi, S.-Y. (2011) High cleavage efficiency of a 2A peptide derived from porcine Teschovirus-1 in human cell lines, Zebrafish and Mice. *PLoS One*, **6**, e18556.
 33. Yao, F., Svensjö, T., Winkler, T., Lu, M., Eriksson, C. and Eriksson, E. (1998) Tetracycline repressor, tetR, rather than the tetR–mammalian cell transcription factor fusion derivatives, regulates inducible gene expression in mammalian cells. *Hum. Gene Ther.*, **9**, 1939–1950.
 34. Nishikura, K. (2010) Functions and regulation of RNA editing by ADAR deaminases. *Annu. Rev. Biochem.*, **79**, 321–349.
 35. Tan, M.H., Li, Q., Shanmugam, R., Piskol, R., Kohler, J., Young, A.N., Liu, K.I., Zhang, R., Ramaswami, G., Ariyoshi, K. *et al.* (2017) Dynamic landscape and regulation of RNA editing in mammals. *Nature*, **550**, 249–254.
 36. Montiel-González, M.F., Vallecillo-Viejo, I.C. and Rosenthal, Joshua J.C. (2016) An efficient system for selectively altering genetic information within mRNAs. *Nucleic Acids Res.*, **44**, e157.
 37. Gott, J.M. and Emeson, R.B. (2000) Functions and mechanisms of RNA editing. *Annu. Rev. Genet.*, **34**, 499–531.
 38. Vogel, P., Schneider, M.F., Wettengel, J. and Stafforst, T. (2014) Improving site-directed RNA editing *in vitro* and in cell culture by chemical modification of the GuideRNA. *Angew. Chem.*, **126**, 6382–6386.
 39. Abudayyeh, O.O., Gootenberg, J.S., Franklin, B., Koob, J., Kellner, M.J., Latha, A., Joung, J., Kirchgatterer, P., Cox, D.B.T. and Zhang, F. (2019) A cytosine deaminase for programmable single-base RNA editing. *Science*, **365**, 382–386.
 40. Sakata, R.C., Ishiguro, S., Mori, H., Tanaka, M., Tatsuno, K., Ueda, H., Yamamoto, S., Seki, M., Masuyama, N., Nishida, K. *et al.* (2020) Base editors for simultaneous introduction of C-to-T and A-to-G mutations. *Nat. Biotechnol.*, **38**, 865–869.
 41. Vallecillo-Viejo, I.C., Liscovitch-Brauer, N., Montiel-Gonzalez, M.F., Eisenberg, E. and Rosenthal, J.J.C. (2018) Abundant off-target edits from site-directed RNA editing can be reduced by nuclear localization of the editing enzyme. *RNA Biol.*, **15**, 104–114.
 42. Rau, K., Rösner, L. and Rentmeister, A. (2019) Sequence-specific m⁶A demethylation in RNA by FTO fused to RCas9. *RNA*, **25**, 1311–1323.
 43. Liu, X.-M., Zhou, J., Mao, Y., Ji, Q. and Qian, S.-B. (2019) Programmable RNA N⁶-methyladenosine editing by CRISPR–Cas9 conjugates. *Nat. Chem. Biol.*, **15**, 865–871.